

Oncocytoma-Like Renal Tumor With Transformation Toward High-Grade Oncocytic Carcinoma

A Unique Case With Morphologic, Immunohistochemical, and Genomic Characterization

Sahussapont J. Sirintrapun, MD, Kim R. Geisinger, MD, Adela Cimic, MD, Anthony Snow, MD, Jill Hagenkord, MD, Federico Monzon, MD, Benjamin L. Legendre Jr, PhD, Anatole Ghazalpour, PhD, Ryan P. Bender, PhD, and Zoran Gatalica, MD, DSc

Abstract: Renal oncocytoma is a benign tumor with characteristic histologic findings. We describe an oncocytoma-like renal tumor with progression to high-grade oncocytic carcinoma and metastasis.

A 74-year-old man with no family history of cancer presented with hematuria. Computed tomography showed an 11 cm heterogeneous multilobulated mass in the right kidney lower pole, enlarged aortocaval lymph nodes, and multiple lung nodules. In the nephrectomy specimen, approximately one third of the renal tumor histologically showed regions classic for benign oncocytoma transitioning to regions of high-grade carcinoma without sharp demarcation.

With extensive genomic investigation using single nucleotide polymorphism-based array virtual karyotyping, multiregion sequencing, and expression array analysis, we were able to show a common lineage between the benign oncocytoma and high-grade oncocytic carcinoma regions in the tumor. We were also able to show karyotypic differences underlying this progression. The benign oncocytoma showed no chromosomal aberrations, whereas the high-grade oncocytic carcinoma showed loss of the 17p region housing FLCN (folliculin [Birt–Hogg–Dubé protein]), loss of 8p, and gain of 8q. Gene expression patterns supported dysregulation and activation of phosphoinositide 3-kinase (PI3K)/v-akt murine thymoma viral oncogene homolog (Akt), mitogen-activated protein kinase (MAPK)/extracellular-signal-regulated kinase (ERK), and mechanistic target

of rapamycin (serine/threonine kinase) (mTOR) pathways in the high-grade oncocytic carcinoma regions. This was partly attributable to FLCN underexpression but further accentuated by overexpression of numerous genes on 8q. In the high-grade oncocytic carcinoma region, vascular endothelial growth factor A along with metalloproteinases matrix metalloproteinase 9 and matrix metalloproteinase 12 were overexpressed, facilitating angiogenesis and invasiveness.

Genetic molecular testing provided evidence for the development of an aggressive oncocytic carcinoma from an oncocytoma, leading to aggressive targeted treatment but eventual death 39 months after the diagnosis.

(*Medicine* 93(15):e81)

Abbreviations: Akt = v-akt murine thymoma viral oncogene homolog, BCL2 = B-cell CLL/lymphoma 2, BRCA1 = breast cancer 1, early onset, cMET = MET proto-oncogene (hepatocyte growth factor receptor), EGFR = epidermal growth factor receptor, ERK = extracellular-signal-regulated kinase, FH = fumarate hydratase, FLCN = folliculin (Birt–Hogg–Dubé protein), HDAC4 = histone deacetylase 4, HIF1A = hypoxia inducible factor 1, KIT = v-kit Hardy-Zuckerman 4 feline sarcoma viral oncogene homolog, MAPK = mitogen-activated protein kinase, MDM2 = MDM2 proto-oncogene, MMP9 = matrix metalloproteinase 9, mTOR = mechanistic target of rapamycin (serine/threonine kinase), MYC (c-Myc) = v-myc avian myelocytomatosis viral oncogene homolog, PDGFRL = platelet-derived growth factor receptor-like, PI3K = phosphoinositide 3-kinase, SRC = SRC proto-oncogene, TSC1 = tuberous sclerosis 1, VEGFA = vascular endothelial growth factor A, VEGFB = vascular endothelial growth factor B, VHL = von Hippel–Lindau tumor suppressor.

Editor: Bo Li.

Received: May 20, 2014; revised: July 22, 2014; accepted: July 26, 2014. From the Department of Pathology, Memorial Sloan Kettering Cancer Center, New York, NY (SJS); University of Mississippi Medical Center, Jackson, MS (KRG); Department of Pathology, Wake Forest Baptist Health, Winston-Salem, NC (AC, AS); 23andMe, Mountain View (JH); Invitae, San Francisco (FM), CA; Transgenomic (BLL); Creighton University School of Medicine (ZG), Omaha, NE; and Caris Life Sciences, Phoenix, AZ (AG, RPB, ZG).

Correspondence: Sahussapont J. Sirintrapun, Department of Pathology, C-509, Memorial Sloan Kettering Cancer Center, 1275 York Avenue, New York, NY 10065 (e-mail: sirintrs@mskcc.org).

The authors have no funding and conflicts of interest to disclose.

AG, RPB, and ZG are employees of Caris Life Sciences (Phoenix, AZ and Dallas, TX); BLL is an employee of Transgenomic, Inc. (Omaha, NE). The other authors have no conflicts of interest to disclose.

Supplemental digital content is available for this article. Direct URL citation appears in the printed text and is provided in the HTML and PDF versions of this article on the journal's Web site (www.md-journal.com).

Copyright © 2014 Wolters Kluwer Health | Lippincott Williams & Wilkins. This is an open access article distributed under the Creative Commons Attribution License 4.0, which permits unrestricted use, distribution, and reproduction in any medium, provided the original work is properly cited.

ISSN: 0025-7974

DOI: 10.1097/MD.0000000000000081

INTRODUCTION

Renal oncocytoma is considered a benign tumor. Microscopically, renal oncocytoma shows nested architecture and tumor cells with granular cytoplasm and round nuclei. The definitive diagnosis of renal oncocytoma requires adequate sampling on kidney resection specimens to exclude regions of solid architecture, nuclear irregularity, and perinuclear cytoplasmic clearing. Such features are seen in eosinophilic chromophobe carcinoma, a malignant tumor that can mimic renal oncocytoma. We present an oncocytoma with transformation to a high-grade oncocytic carcinoma, supported by extensive genomic analysis.

CASE REPORT/CLINICAL HISTORY

The patient is a 74-year-old man with no family history of cancer who presented with hematuria. Computed tomography (CT) showed an 11 cm heterogeneous multilobulated mass in the right kidney lower pole, enlarged aortocaval lymph nodes, and multiple lung nodules. A CT-guided fine needle aspirate (FNA) of an enlarged aortocaval lymph node showed large oncocytic cells with high-grade cytology, which was diagnosed as high-grade carcinoma. A radical nephrectomy with retroperitoneal lymph node dissection was then performed. Subsequently, the patient was placed on Sunitinib that controlled his metastatic disease. After 16 months post operation, the patient was changed to Axitinib and at 20 months post operation, Temozolimumus was added. Although never recurrence free, the patient nearly lived for an additional 20 months; eventually succumbing to his metastatic disease 39 months post operation.

METHODS

Genomic Analysis

Virtual Karyotype With SNP-Based Array Analysis

Tumor enrichment was enabled by selecting only tissue blocks with pure histology. One tissue block contained pure high-grade oncocytic carcinoma with 2 tissue blocks with pure benign oncocytoma-like regions. A matched normal tissue block for germline controls was obtained from adjacent pure normal kidney tissue. After tumor enrichment via manual microdissection, DNA was obtained from 10 μ m paraffin sections as described previously,¹ 15 and 250K Nsp Assay Kits (Affymetrix, Santa Clara, CA) were used according to the manufacturer's protocol, except for increased starting genomic DNA. One microgram of genomic DNA was digested with Nsp restriction enzyme, ligated to adaptors, and amplified by polymerase chain reaction (PCR) using a universal primer. After purification of PCR products with single nucleotide polymorphism (SNP) Clean magnetic beads (Agencourt Biosciences, Beverly, MA), amplicons were quantified, fragmented, labeled, and hybridized to 250K SNP arrays. After washing and staining, the arrays were scanned to generate CEL files for downstream analysis. Data acquired from the Affymetrix Gene-Chip Operating System v4.0 were analyzed using Affymetrix Gene-Chip Genotyping Analysis Software v4.1. Copy number analysis was performed with Copy Number Analyzer for Affymetrix Gene-Chip arrays v3.0, as previously described.¹

Multiregion Gene Sequencing

To validate somatic mutations and estimate mutant allele frequencies, we conducted deep Sanger sequencing. To further exclude another subtype of renal cell carcinoma, sequencing was performed for mutation discovery of known genes involved in renal cell carcinomas. PCR sequences were chosen for the frequently mutated genes in renal cell carcinoma. These genes included VHL (von Hippel–Lindau tumor suppressor), cMET (MET proto-oncogene [hepatocyte growth factor receptor]), FLCN (folliculin [Birt–Hogg–Dubé protein]), and FH (fumarate hydratase) genes. DNA was obtained from 10 μ m paraffin sections from the same tissue blocks used in the SNP-based array analysis. A normal kidney tissue was matched with oncocytoma-like regions and high-grade oncocytic carcinoma.

Microarray Whole Genome mRNA Expression Analysis

Using an Illumina HumanHT-12 v4.0 Whole-Genome cDNA-mediated Annealing, Selection, Extension, and Ligation (DASL) (WGDASL) platform (Illumina, San Diego, CA), expression data were obtained using 29,378 gene probes representing 18,401 known and predicted genes. Both the benign oncocytoma-like regions and the regions of high-grade oncocytic carcinoma were analyzed with the same tumor tissue blocks and matched normal control used in the SNP-based array analysis. Normalization and background subtraction was performed using Genome Studio Software (Illumina). After data normalization, expression ratios of messenger RNA (mRNA) were calculated over the normal control. Overexpression and underexpression were defined as a 2-fold difference when compared with expression values of normal control kidney tissue. Similar expression was when genes had ratios between 0.8 and 1.2 to the normal control kidney tissue.

RESULTS

Morphologic Findings

The initial FNA of an aortocaval lymph node showed large oncocytic cells (red arrows) with anaplastic features (Figure 1A, 20 \times objective). In the resection specimen, approximately one third of the renal tumor histologically showed regions classic for oncocytoma (Figure 1B, 20 \times objective). There was nested architecture and small round cells with round nuclei. Cytoplasmic clearing or nuclear features suggestive of an eosinophilic chromophobe carcinoma were absent. Two thirds of the renal mass showed sheets of high-grade anaplastic cells, atypical mitoses, hemorrhage, and necrosis (Figure 1C, 20 \times objective). These regions of high-grade carcinoma merged with the benign oncocytoma-like regions without any sharp demarcation. Immunohistochemistry for CD10, vimentin, and renal cell carcinoma antigen were entirely negative, arguing against a collision between an oncocytoma and a high-grade clear cell renal cell carcinoma and supporting a progression of the disease. The aortocaval lymph node (Figure 1D, 10 \times objective) showed a metastatic collection of cells (red arrows) morphologically similar to the regions of high-grade oncocytic carcinoma in the renal tumor.

Genomic Analysis

Virtual Karyotype With SNP-Based Array Analysis and Immunohistochemical Support

The benign oncocytoma-like regions (samples 2 and 3 in Figure 2A) showed no significant genomic abnormalities consistent with the morphologic impression of oncocytoma.^{1,2} However, a unique genomic profile was present in the region of high-grade oncocytic carcinoma (sample 1 in Figure 2A). There was a large heterozygous deletion in the region of 17p (blue arrowhead, sample 1 in Figure 2A and region magnification in Figure 2B). The deleted 17p locus included FLCN (at 17p11.2), the gene mutated in Birt–Hogg–Dubé Syndrome (BHDS). There was also a loss of 8p and gain of 8q (red arrowhead, sample 1 in Figure 2A) in the high-grade oncocytic carcinoma. Losses of 8p have been reported in some cases of locally advanced clear cell renal cell carcinoma and metastases.^{3,4} Gains of 8q in renal cell carcinoma have been associated with metastases and poor survival.⁵ In addition, all 3 samples showed 2 incidental

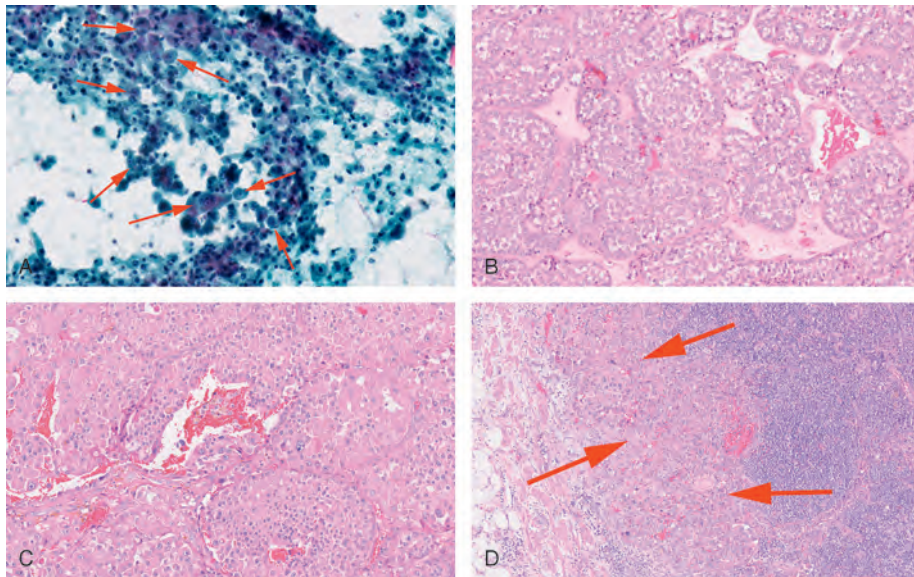


FIGURE 1. (A) FNA of the aortocaval lymph node (20× objective). (B) Benign oncocytoma-like region of the renal tumor (20× objective). (C) High-grade oncocytic carcinoma region of the renal tumor (20× objective). (D) Aortocaval lymph node with metastatic tumor (10× objective). FNA = fine needle aspirate.

regions of autozygosity on 3q and 12p (green arrowheads, samples 1, 2, and 3 in Figure 2A) for which the significance is unknown.

Protein expression of FLCN was explored through immunohistochemistry (Figure 3A and B). The high-grade oncocytic carcinoma region showed decreased protein expression of FLCN (Figure 3A) when compared with the benign oncocytoma-like regions (Figure 3B). This decrease in protein expression appeared to correspond to the heterozygous deletion seen at 17p11.2 on virtual karyotype.

Multiregion Gene Sequencing

The overall findings of multiregion gene sequencing were provided in Table 1. No variant was detected in the VHL, cMET, or FH genes. This supported exclusion of other subtypes of renal cell carcinoma such as clear cell carcinoma, papillary carcinoma, and rare cases of renal cell carcinoma associated with hereditary leiomyomatosis and renal cell

carcinoma. With FLCN, known intronic SNP variants were present in introns 5 and 8. In addition, we detected a known silent polymorphism in exon 11. Neither the high-grade oncocytic carcinoma region nor the oncocytoma-like regions contained any clinically significant mutations.

Microarray Whole Genome mRNA Expression Analysis

Using an Illumina HumanHT-12 v4.0 WGDSL platform, a scatter plot was generated in Figure 4A showing an overview of the expression ratios over the normal control. Supplementary Table S1 (<http://links.lww.com/MD/A35>) provides the raw data. Overall, expression ratios of both tumor regions were concordant further supporting a common lineage to the tumor. Genes showing a 2-fold overexpression in both the benign oncocytoma-like regions and high-grade oncocytic carcinoma regions included several notable genes such as VHL, HIF1A (hypoxia inducible factor 1), cMET,

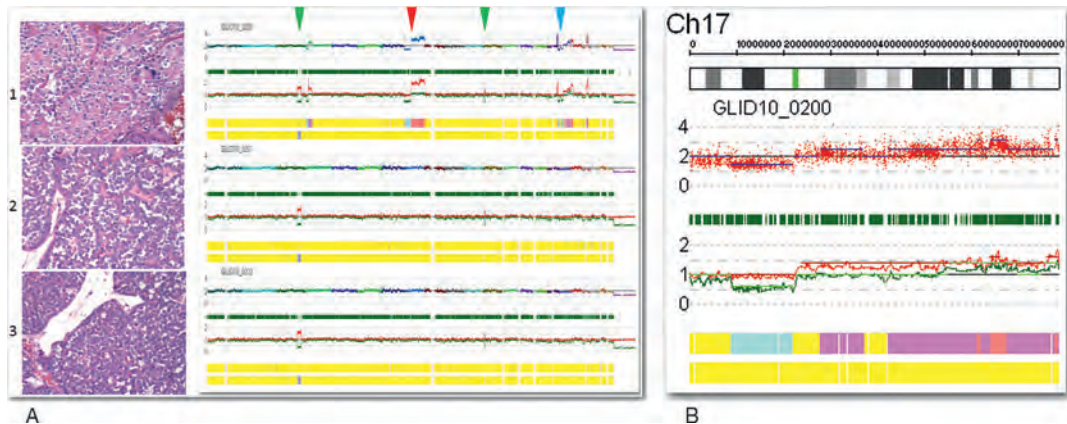


FIGURE 2. (A) Virtual karyotype using SNP-based array analysis. (B) Magnification of the heterozygous deletion in 17p that houses FLCN at 17p11.2. FLCN = folliculin (Birt-Hogg-Dubé protein).

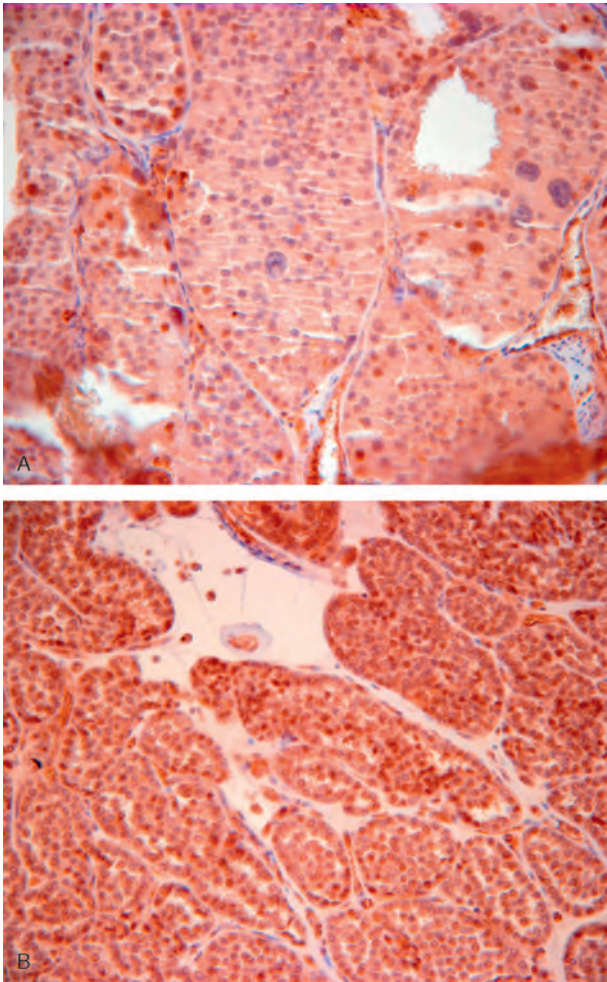


FIGURE 3. (A) and (B) Immunohistochemical FLCN protein expression. (A) High-grade oncocyctic carcinoma. (B) Benign oncocyctoma-like region with slightly higher protein expression of FLCN. FLCN = folliculin (Birt-Hogg-Dubé protein).

and TSC1 (tuberous sclerosis 1), which are cancer genes involved in renal cell carcinoma (Table 2). Other notable genes include BCL2 (B-cell CLL/lymphoma 2), MYC (v-myc avian myelocytomatosis viral oncogene homolog), BRCA1 (breast cancer 1, early onset), and MDM2 (MDM2 proto-oncogene), which are involved in cell death, survival, DNA repair, growth, and proliferation. Commonly overexpressed genes potentially serving as biomarkers for targeted therapy include EGFR (epidermal growth factor receptor), KIT (v-kit Hardy-Zuckerman 4 feline sarcoma viral oncogene homolog), PDGFRL (platelet-derived growth factor receptor-like), VEGFA (vascular endothelial growth factor A), and VEGFB (vascular endothelial growth factor B). The KIT gene showed the highest overexpression.

Despite the overall similarity of gene expression between the 2 tumoral regions, differences were also exhibited. Figure 4B and Supplementary Table S2 (<http://links.lww.com/MD/A36>) show 6 distinct gene subsets: underexpressed in the high-grade oncocyctic carcinoma region but no change in the benign oncocyctoma-like regions (137 gene probes; note that FLCN falls within this section of the dendrogram,

which is consistent with previous SNP array and immunohistochemical results); underexpressed in high-grade oncocyctic carcinoma region and overexpressed in the benign oncocyctoma-like regions (19 gene probes); no change in the high-grade oncocyctic carcinoma region but overexpressed in the benign oncocyctoma-like regions (164 gene probes); no change in the high-grade oncocyctic carcinoma region but underexpressed in the benign oncocyctoma-like regions (154 gene probes); overexpressed in the high-grade oncocyctic carcinoma region and underexpressed in the benign oncocyctoma-like regions (29 gene probes); overexpressed in the high-grade oncocyctic carcinoma region but no change in the benign oncocyctoma-like regions (245 gene probes). Supplementary Table S3 (<http://links.lww.com/MD/A37>) shows a filtered gene probe list derived from subsets 1 and 6 in Supplementary Table S2 (<http://links.lww.com/MD/A36>), which reflect differences in expression in the high-grade oncocyctic carcinoma region but no change in the benign oncocyctoma-like regions. The 8 underexpressed gene probes in subset 1 and 19 overexpressed gene probes in subset 6, corroborates the 8p loss and 8q gain seen on virtual karyotype of the high-grade oncocyctic carcinoma region.

DISCUSSION

The existence of a malignant oncocyctoma has been debated due to general acceptance of renal oncocyctoma as benign. Rare cases of metastatic oncocyctoma have been reported, but these cases may have represented clear cell carcinoma and/or chromophobe carcinoma.^{6,7} A progression from renal oncocyctoma to oncocyctic carcinoma has not yet been reported. The oncocyctic carcinoma region in this tumor showed overwhelming sheet-like growth, desmoplastic stroma, necrosis, marked nondegenerative atypia, and frequent atypical mitoses. Perez-Ordóñez et al⁷ evaluated 70 oncocyctomas and reported no atypical mitoses. Morell-Quadreny et al⁸, described 6 “atypical oncocyctomas” that came closest in appearance to our tumor. These tumors had cellular pleomorphism, transcapsular invasion, and focal necrosis but did not show the confluent necrosis and atypia in our case. A cytogenetic evaluation was performed on these “atypical oncocyctomas” with none of the similar abnormalities of 17p, 8p, or 8q seen in our tumor.⁸

A diagnostic consideration is chromophobe renal cell carcinoma (eosinophilic type), however, the multiple aberrations of chromophobe renal cell carcinoma with loss of chromosomes^{1,2} 1, 2, 6, 10, 13, and 17 were not present in any of the regions of our tumor. Another consideration is the “hybrid oncocyctic/chromophobe” kidney tumor (HOT), as described by Petersson et al.⁹ Such tumors show diffuse hybrid morphology between oncocyctoma and chromophobe with multiple numeric chromosomal aberrations. Our tumor lacked diffuse morphologic changes and rather showed a dichotomous histology with benign oncocyctoma-like regions admixed with high-grade oncocyctic carcinoma regions. HOT also generally behaves in an indolent manner.⁹

The virtual karyotype using SNP-based array analysis allowed us to focus on genomic aberrations found in the regions of high-grade oncocyctic carcinoma, notably the 17p region, which implicated the FLCN gene, along with 8p and 8q where there was a loss and gain, respectively. Through sequencing of genes known to be associated with renal carcinomas, we were able to further argue against a collision tumor with other histologic subtypes. The whole genome

TABLE 1. Multiregion Gene Sequencing for Known Genes Involved With Renal Cell Carcinoma

Client ID Transgenomic ID	Normal 001–143	High-Grade Oncocytic Carcinoma Region 001–144	Oncocytoma-Like Region 001–145
VHL Exon 1	NVD	NVD	NVD
VHL Exon 2	NVD	NVD	NVD
VHL Exon 3	NVD	NVD	NVD
cMET Exon 14	NVD	NVD	NVD
cMET Exon 15	NVD	NVD	NVD
cMET Exon 16	NVD	NVD	NVD
cMET Exon 17	NVD	NVD	NVD
cMET Exon 18	NVD	NVD	NVD
cMET Exon 19	NVD	NVD	NVD
FLCN Exon 4	NVD	NVD	NVD
FLCN Exon 5	NVD	NVD	NVD
FLCN Exon 6	C > T; IVS5-14 (rs1736219), 40% G > A; IVS5-13 (rs3744123), 50%	C > T; IVS5-14 (rs1736219), 40% G > A; IVS5-13 (rs3744123), 50%	C > T; IVS5-14 (rs1736219), 40% G > A; IVS5-13 (rs3744123), 50%
FLCN Exon 7	NVD	NVD	NVD
FLCN Exon 8	NVD	NVD	NVD
FLCN Exon 9	C > T; IVS9+6 (rs8065832), 40%	C > T; IVS9+6 (rs8065832), 50%	C > T; IVS9+6 (rs8065832), 5%
FLCN Exon 10	NVD	NVD	NVD
FLCN Exon 11	c.G > A; p.E411E (rs61750032), 50%	c.G > A; p.E411E (rs61750032), 50%	c.G > A; p.E411E (rs61750032), 70%
FLCN Exon 12	NVD	NVD	NVD
FLCN Exon 13	NVD	NVD	NVD
FLCN Exon 14	NVD	NVD	NVD
FH Exon 1	NVD	NVD	NVD
FH Exon 2	NVD	NVD	NVD
FH Exon 3	NVD	NVD	NVD
FH Exon 4	NVD	NVD	NVD
FH Exon 5	NVD	NVD	NVD
FH Exon 6	NVD	NVD	NVD
FH Exon 7	NVD	NVD	Fail
FH Exon 8	NVD	NVD	NVD
FH Exon 9	NVD	NVD	NVD
FH Exon 10	NVD	NVD	NVD

A = adenine, C = cytosine, cMET = MET proto-oncogene (hepatocyte growth factor receptor), FH = fumarate hydratase, FLCN = folliculin (Birt-Hogg-Dubé protein), G = guanine, ID = identification number, IVS = intervening sequence, NVD = no variant detected, T = thymine, VHL = von Hippel-Lindau tumor suppressor.

microarray expression analysis enabled us to support a common lineage to the benign oncocytoma-like regions and regions of high-grade oncocytic carcinoma.

The heterozygous deletion of the 17p region with FLCN underexpression appears somatic. This contrasts other renal oncocytic tumors “hybrid chromophobe-oncocytomas” of BHDS, which is caused by germline FLCN mutations.¹⁰ BHDS is an autosomal dominant hereditary cancer syndrome caused by germline mutations in FLCN gene. Clinically, it presents with small skin tumors (fibrofolliculomas), pulmonary cysts and renal tumors of which oncocytic and chromophobe types predominate. Evidence for a somatic aberration in our patient are several-fold: the patient lacked a family history suspicious for BHDS and had no FLCN mutation in any tissue analyzed, including normal kidney; only the regions of high-grade oncocytic carcinoma showed the heterozygous deletion of the region housing FLCN on SNP array; FLCN was underexpressed only in the high-grade oncocytic carcinoma region both at the protein and transcript level.

The heterozygous deletion of the 17p region with FLCN underexpression is but 1 factor contributing to the aggressive pathobiology of the high-grade oncocytic carcinoma region.

Mechanistically, the underexpression of FLCN complex in the region of high-grade oncocytic carcinoma would dysregulate ERK (extracellular-signal-regulated kinase)/mTOR (mechanistic target of rapamycin [serine/threonine kinase]) and AMP-activated protein kinase complexes and lead to apoptotic resistance through an aberrant transforming growth factor-β mediated transcription/signaling.^{11–14} FLCN underexpression facilitates invasion through increased MMP9 (matrix metalloproteinase 9) expression.^{11,12} However, the aggressive phenotype demonstrated by this tumor is beyond other low-grade FLCN-mediated renal oncocytic tumors such as HOT “hybrid chromophobe-oncocytomas” of BHDS.⁸ This, in turn, hints at additional contributory mechanisms.

FLCN underexpression increases MMP9 expression which is further potentiated by HDAC4 (histone deacetylase 4) underexpression.^{15,16} Overexpression of an additional metalloproteinase, matrix metalloproteinase 12, further potentiated the invasiveness of high-grade oncocytic carcinoma region. Furthermore, notable overexpressed genes like SRC (SRC proto-oncogene) in the high-grade oncocytic carcinoma region can drive transformation,¹⁷ proliferation, growth,¹⁸ and invasion.¹⁹

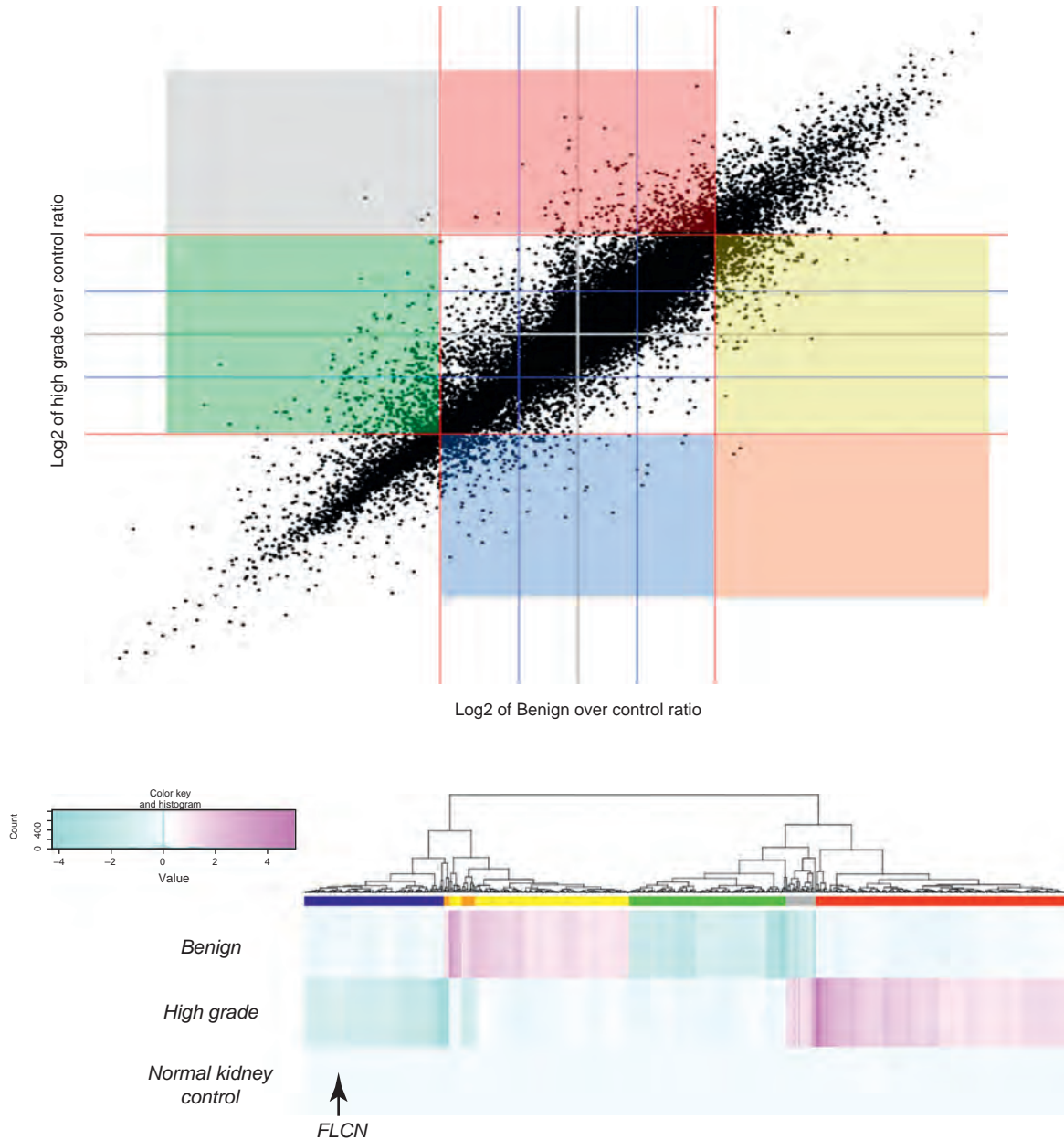


FIGURE 4. (A) Scatter plot of expression data for 29,378 probes. The colored sections represent the following: blue = high-grade downregulated, red = high-grade upregulated, green = benign downregulated, yellow = benign upregulated, grey = high-grade upregulated and benign downregulated, orange = high-grade downregulated and benign upregulated. (B) Hierarchical clustering and heat map of expression ratios for 748 transcripts relative to the normal kidney. The genes falling within the 6 colored sectors in (A) and the gene probes corresponding to the 6 colored bars beneath the dendrogram in (B) represent genes that showed 2-fold overexpression or underexpression in 1 region with the other region having the opposite 2-fold expression or similar expression relative to normal kidney. FLCN = folliculin (Birt-Hogg-Dubé protein).

Using the “Knowledge Base” of Ingenuity Pathway Analysis library (Ingenuity Systems, www.ingenuity.com), the overexpression of genes on 8q (Supplementary Table 3, <http://links.lww.com/MD/A37>) was associated with various cancer types and cell lines with some having roles in invasiveness, proliferation, transformation, progression, PI3K (phosphoinositide 3-kinase), Akt (v-akt murine thymoma viral oncogene homolog), ERK, and nuclear factor of κ light polypeptide gene enhancer in B-cells pathway activation. As such, our global

transcriptomic analysis revealed an even more aggressive phenotype for the high-grade oncocytic carcinoma region than that of HOT “hybrid chromophobe-oncocytomas” of BHDS mediated by FLCN.

Intriguing gene expression patterns present in the benign oncocytoma-like regions were the underexpression of metalloproteinases matrix metalloproteinase 1 and matrix metalloproteinase 7 diminishing invasiveness. Claudin 8, paired box 8,^{20,21} and KIT overexpression in the oncocytoma-like

TABLE 2. Cancer-Related Genes Involved With Renal Cell Carcinoma, Cell Death, Survival, Growth, Proliferation, Tumor Morphology, and Targeted Therapy

Common Cancer-Related Genes	Upregulated Genes	PROBE_ID	Oncocytoma-Like Region	High-Grade Oncocytic Carcinoma Region	
		ILLUMINA	Fold Change	Fold Change	
Cell death, survival, growth, proliferation, and tumor morphology	VHL	ILMN_1738579	24.92	25.04	
	VHL	ILMN_1801984	4.3	4.93	
	VHL	ILMN_2376625	3.87	3.21	
	HIF1A	ILMN_1681283	3.97	2.88	
	cMET	ILMN_1715175	6.29	5	
	PTEN	ILMN_1701134	2.75	2.36	
	TSC1	ILMN_1797367	16.44	9.3	
	TSC1	ILMN_2246510	4.6	3.33	
	BCL2	ILMN_1801119	3.25	3.83	
	BCL2	ILMN_2363250	3.23	2.92	
	MYC	ILMN_2110908	3.47	5.33	
	BRCA1	ILMN_1738027	3.01	3.48	
	BRCA1	ILMN_2311089	3.61	3.97	
	MDM2	ILMN_1736829	9.6	6.68	
	EGFR	ILMN_1696521	6.36	8.32	
	KIT	ILMN_1790160	63.28	43.71	
	Role in targeted therapy	KIT	ILMN_2229379	15.28	26.67
		PDGFR	ILMN_1680339	2.45	4.89
VEGFA		ILMN_2375879	2.84	8.04	
VEGFB		ILMN_1722855	2.09	2.46	

BCL2 = B-cell CLL/lymphoma 2, BRCA1 = breast cancer 1, early onset, cMET = MET proto-oncogene (hepatocyte growth factor receptor), EGFR = epidermal growth factor receptor, HIF1A = hypoxia inducible factor 1, ID = identification number, KIT = v-kit Hardy-Zuckerman 4 feline sarcoma viral oncogene homolog, MDM2 = MDM2 proto-oncogene, MYC = v-myc avian myelocytomatosis viral oncogene homolog, PDGFR = platelet-derived growth factor receptor-like, PTEN = phosphatase and tensin homolog, TSC1 = tuberous sclerosis 1, VEGFA = vascular endothelial growth factor A, VEGFB = vascular endothelial growth factor B, VHL = von Hippel-Lindau tumor suppressor.

regions further corroborated the tumor as being from a renal oncocytoma-like lineage. Interestingly, several cancer-related genes (VHL, HIF1A, cMET, phosphatase and tensin homolog, TSC1, BCL2, BRCA1), which include some tumor suppressors, were also found to be overexpressed in both the benign oncocytoma-like region and the high-grade oncocytic carcinoma region. Although overexpression of some of these genes was predictable for the high-grade oncocytic carcinoma region, overexpression was a puzzling observation for the benign oncocytoma-like regions. There was no database to refer if overexpression of these genes is a consistent finding in renal oncocytoma. It is possible that overexpression of these cancer-related genes could be used to discriminate for malignant potential in renal oncocytoma-like tumors with borderline morphologic features.

Our patient's disease was controlled for close to 3 years while being on tyrosine kinase inhibitors. This was despite a metastatic clinical presentation. The overexpression of EGFR, KIT, PDGFR, VEGFA, VEGFB, would predict for therapeutic effectiveness for these tyrosine kinase inhibitors. With VEGFA, expression was increased >5-fold in the high-grade oncocytic carcinoma region, possibly facilitating angiogenesis further. This may be attributed to several genes (HDAC4,²² SRC,²³ and mothers against DPP homolog²⁴ family member 7), the expression patterns of which would account for upregulation of VEGF. Sunitinib and Axitinib are the 2 drugs that may have the most effect as KIT is one of the overexpressed genes. Because there appears to be a dysregulation/activation of PI3K, Akt, MAPK (mitogen-activated protein

kinase)/ERK, and mTOR pathways in the high-grade oncocytic carcinoma region, the addition of an mTOR inhibitor such as Temsirolimus would provide an additive effect for his targeted therapy. Interestingly, MYC is overexpressed in both the benign oncocytoma-like and high-grade oncocytic carcinoma regions. MYC located on 8q was almost 2-fold higher in the region of high-grade oncocytic carcinoma, and this may have reflected the 8q gain seen on SNP array. MYC overexpression would also predict a therapeutic benefit with specific c-Myc inhibitors or agents that target the MAPK/ERK pathway.⁵

In conclusion, this was the first reported case of a benign oncocytoma transforming to high-grade oncocytic carcinoma, supported by molecular genetic profiling of different tumoral regions that highlighted the importance of tumor heterogeneity in all aspects of patient management. This case report also emphasizes the need for proper sampling and analysis of (histologically) heterogeneous tumor regions. Identification of potentially druggable molecular alterations in different regions and sites may improve patient management and outcomes.^{25,26}

REFERENCES

- Monzon FA, Hagenkord JM, Lyons-Weiler MA, et al. Whole genome SNP arrays as a potential diagnostic tool for the detection of characteristic chromosomal aberrations in renal epithelial tumors. *Mod Pathol.* 2008;21:599–608.
- Hagenkord JM, Gatalica Z, Jonasch E, et al. Clinical genomics of renal epithelial tumors. *Cancer Genet.* 2011;204:285–297.

3. Presti JC Jr, Wilhelm M, Reuter V, et al. Allelic loss on chromosomes 8 and 9 correlates with clinical outcome in locally advanced clear cell carcinoma of the kidney. *J Urol*. 2002;167:1464–1468.
4. Junker K, Romics I, Szendroi A, et al. Genetic profile of bone metastases in renal cell carcinoma. *Eur Urol*. 2004;45:320–324.
5. Klatte T, Kroeger N, Rampersaud EN, et al. Gain of chromosome 8q is associated with metastases and poor survival of patients with clear cell renal cell carcinoma. *Cancer*. 2012;118:5777–5782.
6. Amin MB, Crotty TB, Tickoo SK, et al. Renal oncocytoma: a reappraisal of morphologic features with clinicopathologic findings in 80 cases. *Am J Surg Pathol*. 1997;21:1–12.
7. Perez-Ordóñez B, Hamed G, Campbell S, et al. Renal oncocytoma: a clinicopathologic study of 70 cases. *Am J Surg Pathol*. 1997;21:871–883.
8. Morell-Quadreny L, Gregori-Romero MA, Carda-Batalla C, et al. Renal oncocytomas (typical and atypical variants): a pathologic, immunohistochemical, morphometric, and flow cytometric differential study of 14 cases with cytogenetic support *Int J Surg Pathol*. 1996;3:219–228.
9. Petersson F, Gatalica Z, Grossmann P, et al. Sporadic hybrid oncocytic/chromophobe tumor of the kidney: a clinicopathologic, histomorphologic, immunohistochemical, ultrastructural, and molecular cytogenetic study of 14 cases. *Virchows Arch*. 2010;456:355–365.
10. Kuroda N, Tanaka A, Ohe C, et al. Review of renal oncocytosis (multiple oncocytic lesions) with focus on clinical and pathobiological aspects. *Histol Histopathol*. 2012;27:1407–1412.
11. Pimenta SP, Baldi BG, Nascimento EC, et al. Birt–Hogg–Dubé syndrome: metalloproteinase activity and response to doxycycline. *Clinics (Sao Paulo)*. 2012;67:1501–1504.
12. Nishii T, Tanabe M, Tanaka R, et al. Unique mutation, accelerated mTOR signaling and angiogenesis in the pulmonary cysts of Birt–Hogg–Dubé syndrome. *Pathol Int*. 2013;63:45–55.
13. Cash TP, Gruber JJ, Hartman TR, et al. Loss of the Birt–Hogg–Dubé tumor suppressor results in apoptotic resistance due to aberrant TGF β -mediated transcription. *Oncogene*. 2011;30:2534–2546.
14. Klomp JA, Petillo D, Niemi NM, et al. Birt–Hogg–Dubé renal tumors are genetically distinct from other renal neoplasias and are associated with up-regulation of mitochondrial gene expression. *BMC Med Genomics*. 2010;3:59.
15. Qin L, Han YP. Epigenetic repression of matrix metalloproteinases in myofibroblastic hepatic stellate cells through histone deacetylases 4: implication in tissue fibrosis. *Am J Pathol*. 2010;177:1915–1928.
16. Bonacci G, Schopfer FJ, Batthyany CI, et al. Electrophilic fatty acids regulate matrix metalloproteinase activity and expression. *J Biol Chem*. 2011;286:16074–16081.
17. Kadono Y, Okada Y, Namiki M, et al. Transformation of epithelial Madin-Darby canine kidney cells with p60(v-src) induces expression of membrane-type 1 matrix metalloproteinase and invasiveness. *Cancer Res*. 1998;58:2240–2244.
18. Murillo MM, Castillo GD, Sánchez A, et al. Involvement of EGF receptor and c-Src in the survival signals induced by TGF- β 1 in hepatocytes. *Oncogene*. 2005;24:4580–4587.
19. Rodrigues S, Attoub S, Nguyen QD, et al. Selective abrogation of the proinvasive activity of the trefoil peptides pS2 and spasmolytic polypeptide by disruption of the EGF receptor signaling pathways in kidney and colonic cancer cells. *Oncogene*. 2003;22:4488–4497.
20. Osunkoya AO, Cohen C, Lawson D, et al. Claudin-7 and claudin-8: immunohistochemical markers for the differential diagnosis of chromophobe renal cell carcinoma and renal oncocytoma. *Hum Pathol*. 2009;40:206–210.
21. Hu Y, Hartmann A, Stoehr C, et al. PAX8 is expressed in the majority of renal epithelial neoplasms: an immunohistochemical study of 223 cases using a mouse monoclonal antibody. *J Clin Pathol*. 2012;65:254–256.
22. Geng H, Harvey CT, Pittsenbarger J, et al. HDAC4 protein regulates HIF1 α protein lysine acetylation and cancer cell response to hypoxia. *J Biol Chem*. 2011;286:38095–38102.
23. Jiang BH, Agani F, Passaniti A, et al. V-SRC induces expression of hypoxia-inducible factor 1 (HIF-1) and transcription of genes encoding vascular endothelial growth factor and enolase 1: involvement of HIF-1 in tumor progression. *Cancer Res*. 1997;57:5328–5335.
24. Nam EH, Park SR, Kim PH. TGF- β 1 induces mouse dendritic cells to express VEGF and its receptor (Flt-1) under hypoxic conditions. *Exp Mol Med*. 2010;42:606–613.
25. Gerlinger M, Rowan AJ, Horswell S, et al. Intratumor heterogeneity and branched evolution revealed by multiregion sequencing. *N Engl J Med*. 2012;366:883–892.
26. Longo DL. Tumor heterogeneity and personalized medicine. *N Engl J Med*. 2012;366:956–957.